IEICE TRANS. FUNDAMENTALS, VOL.E84–A, NO.9 SEPTEMBER 2001

PAPER

Analysis of Chaotic Phenomena in Two RC Phase Shift Oscillators Coupled by a Diode

Yasuteru HOSOKAWA[†,††a)], ***Student Member***, **Yoshifumi NISHIO**[†*], ***and*** **Akio USHIDA**[†], ***Regular Members***

SUMMARY In this paper, a simple chaotic circuit using two RC phase shift oscillators and a diode is proposed and analyzed. By using a simpler model of the original circuit, the mechanism of generating chaos is explained and the exact solutions are derived. The exact expression of the Poincaré map and its Jacobian matrix make it possible to confirm the generation of chaos using the Lyapunov exponents and to investigate the related bifurcation phenomena.

key words: *chaos, RC phase shift oscillator, diode, torus, piecewise-linear analysis*

1. Introduction

There have been many investigations on various kinds of applications of chaos. For instance, chaos communication systems [1], [2], chaos neural networks [3], [4], spatio-temporal behavior in coupled chaotic circuits systems [5], [6] and so on. In order to design chaos communication systems using chaos synchronization, it is necessary to make almost identical chaotic circuits. Only IC realization of the circuit would make it possible. Further, realization of large-scale of chaotic circuits networks would be possible only on IC chip. Therefore, it is considered to be important to study on IC chip design of chaotic circuits [7]–[10]. One of the most important subject on such studies is how small is the circuit, namely how many transistors are needed to construct one chaotic circuit. Until now, OTA is used in almost these studies [11] for realization of negative resistor, gyrator and so on. Hysteresis or saturation characteristics of OTA is also exploited as a part of nonlinear elements. However, an OTA is usually realized by using several numbers of transistors. As a result, chaotic circuits including OTAs are not so small.

In this paper, we design a new chaotic circuit using two RC phase shift oscillators and a diode and analyze the circuit using a simpler model. This circuit consists of only some diodes, transistors, resistors and capacitors, namely we do not have to realize any elements in the circuit by some circuits including OTAs. We show the simple circuit exhibits chaos by circuit experiments. In order to make clear the mechanism of generating chaos and to investigate related bifurcation, we derive a simpler model from the original circuit. In the simpler model transistors are modeled by linearized ones and a coupling diode is modeled by two-segment piecewise-linear characteristics. This makes us possible to explain the generation of chaos and to derive exact solutions of the circuit. It is also possible to derive the exact expression of the Poincaré map and its Jacobian matrix. We can calculate the Lyapunov exponent using the Jacobian matrix.

In the Sect. 2 the circuit model and circuit experimental results are shown. In the Sect. 3 we derive the simpler model from the original circuit and show the computer calculated results using exact solutions of the simpler model. We can explain the mechanism of generating chaos. In the Sect. 4 the Poincaré map is defined and the Lyapunov exponent is calculated. They confirm the generation of chaos and show the detailed bifurcation scenario. Some concluding remarks is presented in the Sect. 5.

2. Circuit Set-up

Figure 1(a) shows a well-known simple RC phase shift oscillator which consists of a third order RC ladder network and a feedback amplifier. Figure 1(b) shows a typical wave form of the voltage observed from the RC phase shift oscillator. In this oscillator, the amplitude of the oscillation does not become so large, because it is controlled by turn-on of the transistor. Hence, if we need oscillation with larger amplitude, we have to modify the circuit.

Figure 2(a) shows a modified RC phase shift oscillator with level shift diodes. Figure 2(b) shows a typical wave form of the voltage observed from the modified RC phase shift oscillator with level shift diodes. We can see the amplitude becomes larger by the level shift diodes.

Figure 3 shows our circuit model. In this circuit, two RC phase shift oscillators with level shift diodes are coupled by a diode D_0. In the beginning we carried out circuit experiments for a similar circuit without level shift diodes. But, we could not observe any

Manuscript received December 18, 2000.

[†]The authors are with the Faculty of Engineering, Tokushima University, Tokushima-shi, 770-8506 Japan.

[††]The author is with the Faculty of Management and Information Science, Shikoku University, Tokushima-shi, 771-1192 Japan.

[*]Presently, the author is with the Department of Communication Systems, Swiss Federal Institute of Technology Lausanne (EPFL), Switzerland.

a) E-mail: hosokawa@ee.tokushima-u.ac.jp

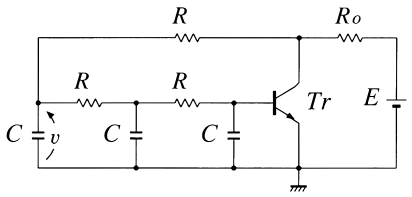

(a)

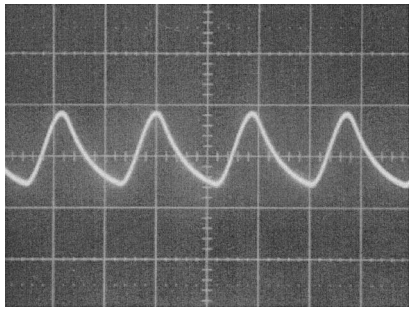

(b)

Fig. 1 (a) RC phase shift oscillator. (b) Typical wave form. Horizontal axis is 10 [μs/div]. Vertical axis is 0.5 [V/div]. R_o = 2.00 [kΩ], R = 2.00 [kΩ], C = 4.70 [nF] and E = 15.0 [V].

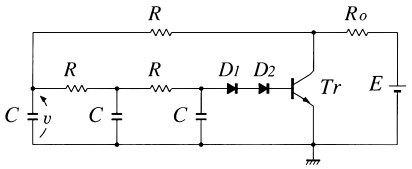

(a)

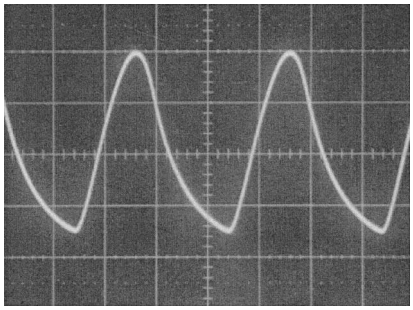

(b)

Fig. 2 (a) RC phase shift oscillator with level shift diodes. (b) Typical wave form. Horizontal axis is 10 [μs/div]. Vertical axis is [0.5V/div]. R_o = 2.00 [kΩ], R = 2.00 [kΩ], C = 4.70 [nF] and E = 15.0 [V].

chaotic oscillations. We considered that it was because the amplitude of the oscillation of each RC phase shift oscillator was too small to exploiting nonlinearity of the coupling diode. That's why we added level shift diodes to the RC phase shift oscillators. As a result, we not only observed chaotic oscillations but also understood that the nonlinearity of the transistors did not play any roles of generating chaos. We explain about this in the next section.

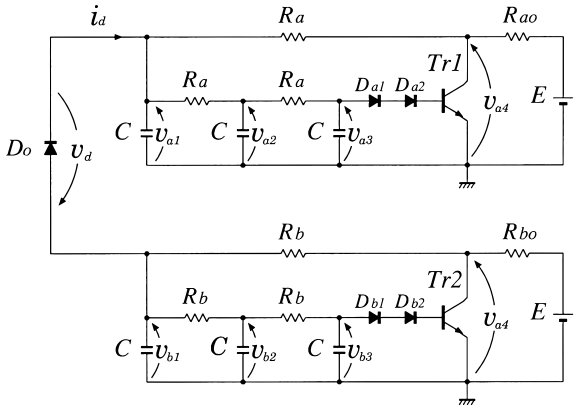

Fig. 3 RC-Transistor chaotic circuit.

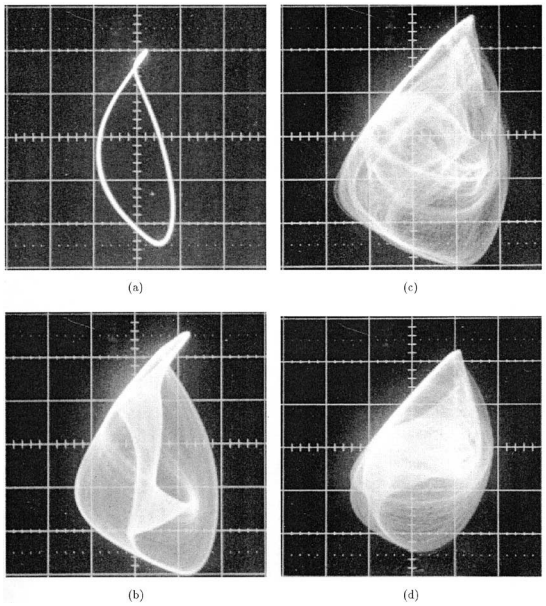

Fig. 4 Typical examples of attractors obtained from the circuit in Fig. 3. Horizontal axis is v_{a1} (0.2 [V/div]) and vertical axis is v_{b1} (0.2 [V/div]). R_{ao} = 6.47 [kΩ], R_a = 0.820 [kΩ], R_b = 2.00 [kΩ] and C = 4.70 [nF]. (a) R_{bo} = 2.00 [kΩ], (b) R_{bo} = 1.88 [kΩ], (c) R_{bo} = 1.85 [kΩ], (d) R_{bo} = 1.58 [kΩ].

Figure 4 shows typical examples of attractors obtained by circuit experiments. We choose R_{bo} as a control parameter which is varied in 1.58 [kΩ] $< R_{bo} <$ 2.00 [kΩ]. Other parameter values are fixed as R_{ao} = 6.47 [kΩ], R_a = 0.820 [kΩ], R_b = 2.00 [kΩ] and C = 4.70 [nF], respectively. The BJT is type 2SC1815.

We can see periodic orbit (a), quasi-periodic orbit (b) and complex attractors being looked chaotic (c), (d).

This circuit consist of only two simple RC phase shift oscillators and a diode. Namely, neither inductors nor negative resistors are included. Therefore, it is considered to be realized on the IC chip without complication.

However, it is too difficult to analyze this circuit

as it is, because this circuit includes many nonlinear elements. Therefore, it is impossible to make clear the mechanism of generating chaos. This means that we can not maintain that chaos will be observed if we replace, for example, the transistor by another one. Because there is possibility that very slight something of the element may play important role to generate chaos. We do not consider that such a circuit is very useful for future applications.

3. Linearized Model

In this section, in order to make clear the mechanism of generating chaos and to investigate related bifurcation, we derive a simple linearized model of the circuit model in Fig. 3.

First of all, the transistors with two level-shift diodes in the circuit are assumed to operate as ideal linear elements as shown in Fig. 5, namely

$$\begin{aligned} i_B &= \frac{1}{R_t}(v_{BE} - V_B) \\ i_C &= \beta_F i_B \end{aligned} \tag{1}$$

where β_F is the forward current gain of the device. This approximation is signified forward active region only.

Next, the $v-i$ characteristics of the diode coupling two RC phase oscillators are approximated by the following two-segment piecewise-linear function shown in Fig. 6,

$$i_d = \begin{cases} \dfrac{1}{R_d}(v_d - V_{th}) & (v_d > V_{th}) \\ 0 & (v_d \le V_{th}). \end{cases} \tag{2}$$

By using the above simplified transistors and diode, the circuit equations are described as follows:

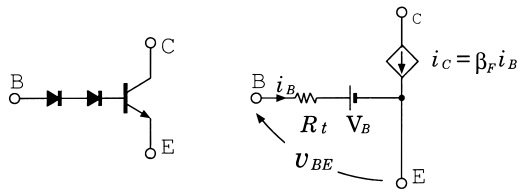

Fig. 5 BJT model.

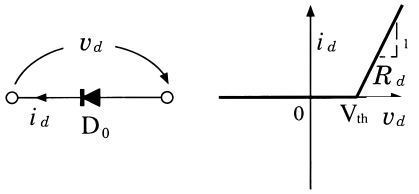

Fig. 6 Diode model.

$$\begin{aligned}
R_aC\frac{dv_{a1}}{dt} &= \left(\frac{R_{ao}}{R_{ao}+R_a} - 2\right)v_{a1} + v_{a2} \\
&\quad - \frac{R_{ao}R_a\beta_F}{(R_{ao}+R_a)\,R_t}v_{a3} - \frac{R_{ao}R_a\beta_F}{(R_{ao}+R_a)\,R_t}V_B \\
&\quad - \frac{R_a}{R_{ao}+R_a}E + R_a i_d \\
R_aC\frac{dv_{a2}}{dt} &= v_{a1} - 2v_{a2} + v_{a3} \\
R_aC\frac{dv_{a3}}{dt} &= v_{a2} - \left(\frac{R_a}{R_t} + 1\right)v_{a3} - \frac{R_a}{R_t}V_B \\
R_bC\frac{dv_{b1}}{dt} &= \left(\frac{R_{bo}}{R_{bo}+R_b} - 2\right)v_{b1} + v_{b2} \\
&\quad - \frac{R_{bo}R_b\beta_F}{(R_{bo}+R_b)\,R_t}v_{b3} - \frac{R_{bo}R_b\beta_F}{(R_{bo}+R_b)\,R_t}V_B \\
&\quad - \frac{R_b}{R_{bo}+R_b}E - R_b i_d \\
R_bC\frac{dv_{b2}}{dt} &= v_{b1} - 2v_{b2} + v_{b3} \\
R_bC\frac{dv_{b3}}{dt} &= v_{b2} - \left(\frac{R_b}{R_t} + 1\right)v_{b3} - \frac{R_b}{R_t}V_B.
\end{aligned} \tag{3}$$

By changing the variables and parameters,

$$v_{ak} = V_{th}x_{ak}, \quad v_{bk} = V_{th}x_{bk}, \quad (k = 1, 2, 3),$$

$$\alpha_a = \frac{R_{ao}}{R_{ao}+R_a}, \quad \alpha_b = \frac{R_{bo}}{R_{bo}+R_b},$$

$$\beta_a = \frac{R_aE}{R_{ao}V_{th}}, \quad \beta_b = \frac{R_bE}{R_{bo}V_{th}}, \quad \gamma = \frac{R_a}{R_t},$$

$$\delta = \frac{V_B}{V_{th}}, \quad \varepsilon = \frac{R_a}{R_b}, \quad \zeta = \frac{R_a}{R_d}, \quad t = R_aC\tau, \tag{4}$$

the normalized circuit equations are described by the following six-dimensional piecewise-linear differential equations.

$$\begin{aligned}
\dot{x}_{a1} &= (\alpha_a - 2)x_{a1} + x_{a2} - \alpha_a\gamma\beta_F x_{a3} \\
&\quad + \alpha_a\gamma\beta_F\delta + \alpha_a\beta_a + \zeta y_d \\
\dot{x}_{a2} &= x_{a1} - 2x_{a2} + x_{a3} \\
\dot{x}_{a3} &= x_{a2} - (\gamma + 1)x_{a3} + \gamma\delta \\
\dot{x}_{b1} &= \varepsilon(\alpha_b - 2)x_{b1} + \varepsilon x_{b2} - \alpha_b\gamma\beta_F x_{b3} \\
&\quad + \alpha_b\gamma\beta_F\delta + \alpha_b\beta_b\varepsilon - \zeta y_d \\
\dot{x}_{b2} &= \varepsilon(x_{b1} - 2x_{b2} + x_{b3}) \\
\dot{x}_{b3} &= \varepsilon x_{b2} - (\gamma + \varepsilon)x_{b3} + \gamma\delta
\end{aligned} \tag{5}$$

where y_d is a piecewise-linear function corresponding

to the $v-i$ characteristics of the coupling diode and is described as

$$y_d = \begin{cases} x_{b1} - x_{a1} - 1 & \text{for } x_{b1} - x_{a1} > 1 \\ 0 & \text{for } x_{b1} - x_{a1} \leq 1. \end{cases} \tag{6}$$

Since the circuit equations (5) are piecewise-linear, exact solutions in each linear region can be derived. At first, we define two piecewise-linear regions as follows.

$$\begin{array}{ll} \mathbf{R_1}: & x_{b1} - x_{a1} > 1 \\ \mathbf{R_0}: & x_{b1} - x_{a1} \leq 1. \end{array} \tag{7}$$

Namely, $\mathbf{R_1}$ corresponds to the region where the coupling diode is ON, while $\mathbf{R_0}$ corresponds to OFF. Note that in $\mathbf{R_0}$ the circuit equations are completely decoupled into two three-dimensional equations.

We calculate the eigenvalues in each region from Eq. (5). The eigenvalues in each region are described as follows.

$$\begin{array}{ll} \mathbf{R_1}: & \lambda_{11}, \lambda_{12}, \lambda_{13}, \lambda_{14}, \sigma_1 \pm j\omega_1 \\ \mathbf{R_0}: & \lambda_a, \sigma_a \pm j\omega_a, \lambda_b, \sigma_b \pm j\omega_b. \end{array} \tag{8}$$

The eigenvalues in $\mathbf{R_1}$ are obtained numerically from the 6th order eigenequation of Eq. (5). On the other hand, $\lambda_a, \sigma_a \pm j\omega_a$ can be derived from

$$\begin{vmatrix} \lambda - (\alpha_a - 2) & -1 & \alpha_a\gamma\beta_F \\ -1 & \lambda + 2 & -1 \\ 0 & -1 & \lambda + \gamma + 1 \end{vmatrix} = 0 \tag{9}$$

and $\lambda_b, \sigma_b \pm j\omega_b$ can be derived from

$$\begin{vmatrix} \lambda - \varepsilon(\alpha_b - 2) & -\varepsilon & \alpha_b\gamma\beta_F \\ -\varepsilon & \lambda + 2\varepsilon & -\varepsilon \\ 0 & -\varepsilon & \lambda + \gamma + \varepsilon \end{vmatrix} = 0 \tag{10}$$

by virtue of the decoupling.

Next we define the equilibrium points in $\mathbf{R_1}$ and $\mathbf{R_0}$ as

$$\mathbf{E_1} = \begin{bmatrix} E_{1a1} \\ E_{1a2} \\ E_{1a3} \\ E_{1b1} \\ E_{1b2} \\ E_{1b3} \end{bmatrix} \quad \text{and} \quad \mathbf{E_0} = \begin{bmatrix} E_{0a1} \\ E_{0a2} \\ E_{0a3} \\ E_{0b1} \\ E_{0b2} \\ E_{0b3} \end{bmatrix}, \tag{11}$$

respectively. These values are calculated by putting the right side of Eq. (5) to be equal to zero.

Then, we can describe the exact solutions in each linear region as follows.

$\mathbf{R_1}$: Diode is ON.

$$\mathbf{x}(\tau) - \mathbf{E_1} = \mathbf{F}(\tau) \cdot \mathbf{F}^{-1}(0) \cdot (\mathbf{x}(0) - \mathbf{E_1}),$$

$$\mathbf{x}(\tau) = \begin{bmatrix} x_{a1}(\tau) \\ x_{a2}(\tau) \\ x_{a3}(\tau) \\ x_{b1}(\tau) \\ x_{b2}(\tau) \\ x_{b3}(\tau) \end{bmatrix}, \quad \mathbf{F}(\tau) = \begin{bmatrix} \mathbf{f_{a1}}(\tau) \\ \mathbf{f_{a2}}(\tau) \\ \mathbf{f_{a3}}(\tau) \\ \mathbf{f_{b1}}(\tau) \\ \mathbf{f_{b2}}(\tau) \\ \mathbf{f_{b3}}(\tau) \end{bmatrix},$$

$$\mathbf{f_{a3}}(\tau) = \begin{bmatrix} e^{\lambda_{11}\tau} \\ e^{\lambda_{12}\tau} \\ e^{\lambda_{13}\tau} \\ e^{\lambda_{14}\tau} \\ e^{\sigma_1\tau}\cos\omega_1\tau \\ e^{\sigma_1\tau}\sin\omega_1\tau \end{bmatrix},$$

$$\mathbf{f_{a2}}(\tau) = \frac{d\mathbf{f_{a3}}(\tau)}{d\tau} + (\gamma+1)\mathbf{f_{a3}}(\tau),$$

$$\mathbf{f_{a1}}(\tau) = \frac{d\mathbf{f_{a2}}(\tau)}{d\tau} + 2\mathbf{f_{a2}}(\tau) - \mathbf{f_{a3}}(\tau). \tag{12}$$

We omit the description of $\mathbf{f_{bk}}$ (k=1,2,3), because it is complicated enough to write here in spite of the solutions of linear algebraic equations.

$\mathbf{R_0}$: Diode is OFF.

$$\mathbf{x_a}(\tau) - \mathbf{E_{0a}} = \mathbf{G_a}(\tau) \cdot \mathbf{G_a}^{-1}(0) \cdot (\mathbf{x_a}(0) - \mathbf{E_{0a}}),$$

$$\mathbf{x_b}(\tau) - \mathbf{E_{0b}} = \mathbf{G_b}(\tau) \cdot \mathbf{G_b}^{-1}(0) \cdot (\mathbf{x_b}(0) - \mathbf{E_{0b}}),$$

$$\mathbf{x_a}(\tau) = \begin{bmatrix} x_{a1}(\tau) \\ x_{a2}(\tau) \\ x_{a3}(\tau) \end{bmatrix}, \quad \mathbf{x_b}(\tau) = \begin{bmatrix} x_{b1}(\tau) \\ x_{b2}(\tau) \\ x_{b3}(\tau) \end{bmatrix},$$

$$\mathbf{E_{0a}} = \begin{bmatrix} E_{0a1} \\ E_{0a2} \\ E_{0a3} \end{bmatrix}, \quad \mathbf{E_{0b}} = \begin{bmatrix} E_{0b1} \\ E_{0b2} \\ E_{0b3} \end{bmatrix},$$

$$\mathbf{G_a}(\tau) = \begin{bmatrix} \mathbf{g_{a1}}(\tau) \\ \mathbf{g_{a2}}(\tau) \\ \mathbf{g_{a3}}(\tau) \end{bmatrix}, \quad \mathbf{G_b}(\tau) = \begin{bmatrix} \mathbf{g_{b1}}(\tau) \\ \mathbf{g_{b2}}(\tau) \\ \mathbf{g_{b3}}(\tau) \end{bmatrix},$$

$$\mathbf{g_{a3}}(\tau) = \begin{bmatrix} e^{\lambda_a\tau} \\ e^{\sigma_a\tau}\cos\omega_a\tau \\ e^{\sigma_a\tau}\sin\omega_a\tau \end{bmatrix},$$

$$\mathbf{g_{a2}}(\tau) = \frac{d\mathbf{g_{a3}}(\tau)}{d\tau} + (\gamma+1)\mathbf{g_{a3}}(\tau),$$

$$\mathbf{g_{a1}}(\tau) = \frac{d\mathbf{g_{a2}}(\tau)}{d\tau} + 2\mathbf{g_{a2}}(\tau) - \mathbf{g_{a3}}(\tau),$$

$$\mathbf{g_{b3}}(\tau) = \begin{bmatrix} e^{\lambda_b\tau} \\ e^{\sigma_b\tau}\cos\omega_b\tau \\ e^{\sigma_b\tau}\sin\omega_b\tau \end{bmatrix},$$

$$\mathbf{g_{b2}}(\tau) = \frac{1}{\varepsilon}\frac{d\mathbf{g_{b3}}(\tau)}{d\tau} + \frac{\gamma+1}{\varepsilon}\mathbf{g_{b3}}(\tau),$$

$$\mathbf{g_{b1}}(\tau) = \frac{1}{\varepsilon}\frac{d\mathbf{g_{b2}}(\tau)}{d\tau} + 2\mathbf{g_{b2}}(\tau) - \mathbf{g_{b3}}(\tau). \tag{13}$$

Figure 7(1) shows computer calculated results of the exact solutions in Eqs. (12) and (13). We choose α_b as the control parameter and other parameters are fixed as $\alpha_a = 0.80$, $\beta_a = 5.71$, $\beta_b = 3.21$, $\gamma = 0.267$, $\delta = 3.00$,

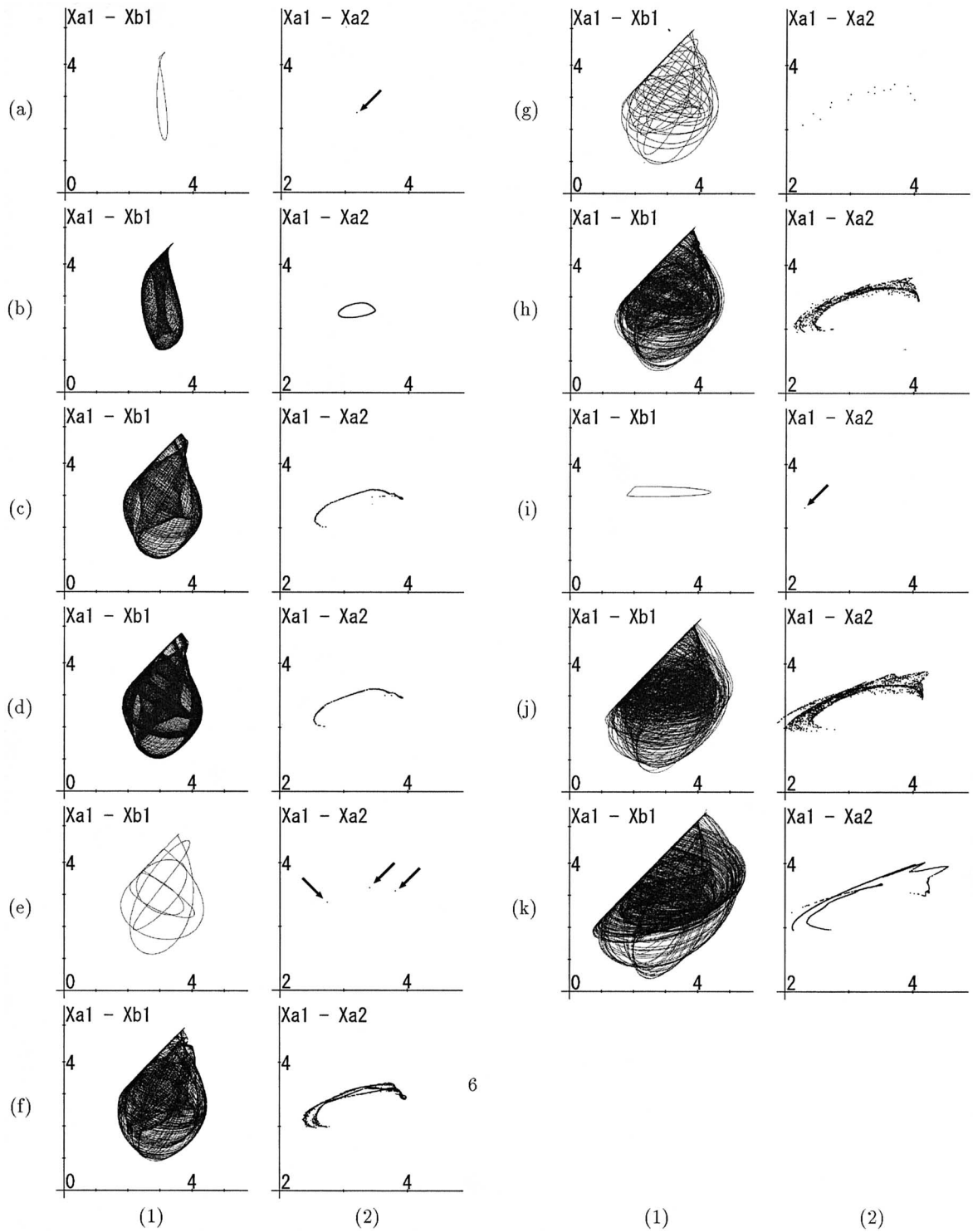

Fig. 7 Computer calculated results. (1) Attractors. (2) Poincaré map. $\alpha_a = 0.80$, $\beta_a = 5.71$, $\beta_b = 3.21$, $\gamma = 0.267$, $\delta = 3.00$, $\varepsilon = 0.670$, $\zeta = 60.0$, and $\beta_F = 100$. (a) $\alpha_b = 0.700$, (b) $\alpha_b = 0.750$, (c) $\alpha_b = 0.815$, (d) $\alpha_b = 0.817$, (e) $\alpha_b = 0.825$, (f) $\alpha_b = 0.832$, (g) $\alpha_b = 0.848$, (h) $\alpha_b = 0.860$, (i) $\alpha_b = 0.865$, (j) $\alpha_b = 0.880$, (k) $\alpha_b = 0.902$.

$\varepsilon = 0.670$, $\zeta = 60.0$, and $\beta_F = 100$. We can observe almost same attractors and the same bifurcation scenario as those observed from circuit experiments. Namely, our linearized model does not lose important features of the original circuit. This means that the RC phase shift oscillators in the original circuit behave as simple divergently oscillating parts and that only the nonlinearity of the coupling diode controls the amplitude. In

other words, the RC phase oscillators play a role of *expanding*, while the coupling diode plays a role of *folding*. These two features, expanding and folding, are known as the essence of generating chaos. From the result we can now maintain that our circuit model is enough to be robust to generate chaos, because the RC phase shift oscillators do not have to possess any special characteristics, but they have only to oscillate divergently.

This result also encourages us to establish a designing method of chaos-generating circuits in a simple way, for example just to replace RC phase oscillators by another types of oscillators. Such designing method of chaos-generating circuits would contribute to realize engineering applications of chaos and our most important future research.

4. Poincaré Map

In order to confirm the generation of chaos and to investigate bifurcation scenario, we derive the Poincaré map.

Let us define the following subspace

$$\mathbf{S} = \mathbf{S_1} \cap \mathbf{S_2} \tag{14}$$

where

$$\begin{aligned} &\mathbf{S_1} : x_{b1} - x_{a1} = 1 \\ &\mathbf{S_2} : \{\varepsilon(\alpha_b - 2)x_{b1} + \varepsilon x_{b2} - \alpha_b\gamma\beta_F x_{b3} \\ &\quad +\alpha_b\gamma\beta_F\delta + \alpha_b\beta_b\varepsilon\} - \{(\alpha_a - 2)x_{a1} \\ &\quad +x_{a2} - \alpha_a\gamma\beta_F x_{a3} + \alpha_a\gamma\beta_F\delta + \alpha_a\beta_a\} \\ &\quad > 0. \end{aligned} \tag{15}$$

The subspace $\mathbf{S_1}$ corresponds to the boundary condition between $\mathbf{R_1}$ and $\mathbf{R_0}$, while the subspace $\mathbf{S_2}$ corresponds to the condition $\dot{x}_{b1} - \dot{x}_{a1} > 0$. Namely, $\mathbf{S}$ corresponds to the transitional condition from $\mathbf{R_0}$ to $\mathbf{R_1}$.

Let us consider the solution starting form an initial point on $\mathbf{S}$. The solution returns back to $\mathbf{S}$ again after wandering $\mathbf{R_1}$ and $\mathbf{R_0}$ as shown in Fig. 8. Hence, we can derive the Poincaré map as follows.

$$\mathbf{T} : \ \mathbf{S} \to \mathbf{S}, \ \mathbf{x_0} \mapsto \mathbf{T}(\mathbf{x_0}) \tag{16}$$

where $\mathbf{x_0}$ is an initial point on $\mathbf{S}$, while $\mathbf{T}(\mathbf{x_0})$ is the point at which the solution starting from $\mathbf{x_0}$ hits $\mathbf{S}$ again.

The concrete representation of $\mathbf{T}(\mathbf{x_0})$ is given as

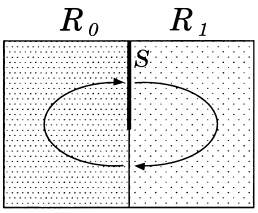

Fig. 8 Derivation of the Poincaré map.

follows using the exact solutions in Eqs. (12) and (13).

Suppose that the solution starting from $\mathbf{x_0}$=(X_{a10}, X_{a20}, X_{a30}, $X_{a10}+1$, X_{b20}, X_{b30}) when $\tau = 0$ hits $\mathbf{S_1}$ and enters $\mathbf{R_0}$ at $\mathbf{x_1}$=(X_{a11}, X_{a21}, X_{a31}, X_{a11}+1, X_{b21}, X_{b31}) when $\tau = \tau_1$. In this case, $\mathbf{x_1}$ is given by

$$\begin{aligned} &\begin{bmatrix} X_{a11} - E_{1a1} \\ X_{a21} - E_{1a2} \\ X_{a31} - E_{1a3} \\ X_{a11} + 1 - E_{1b1} \\ X_{b21} - E_{1b2} \\ X_{b31} - E_{1b3} \end{bmatrix} \\ &= \mathbf{F}(\tau_1) \cdot \mathbf{F}^{-1}(0) \cdot \begin{bmatrix} X_{a10} - E_{1a1} \\ X_{a20} - E_{1a2} \\ X_{a30} - E_{1a3} \\ X_{a10} + 1 - E_{1b1} \\ X_{b20} - E_{1b2} \\ X_{b30} - E_{1b3} \end{bmatrix} \end{aligned} \tag{17}$$

where τ_1 is given by using the first and fourth rows of Eq. (17). The solution hits $\mathbf{S}$ again at $\mathbf{x_2}$=(X_{a12}, X_{a22}, X_{a32}, $X_{a12}+1$, X_{b22}, X_{b32}) when $\tau = \tau_1 + \tau_2$. $\mathbf{x_2}$ is given by

$$\begin{aligned} &\begin{bmatrix} X_{a12} - E_{0a1} \\ X_{a22} - E_{0a2} \\ X_{a32} - E_{0a3} \end{bmatrix} \\ &= \mathbf{G_a}(\tau_2) \cdot {\mathbf{G_a}}^{-1}(0) \cdot \begin{bmatrix} X_{a11} - E_{0a1} \\ X_{a21} - E_{0a2} \\ X_{a31} - E_{0a3} \end{bmatrix} \\ &\begin{bmatrix} X_{a12} + 1 - E_{0b1} \\ X_{b22} - E_{0b2} \\ X_{b32} - E_{0b3} \end{bmatrix} \\ &= \mathbf{G_b}(\tau_2) \cdot {\mathbf{G_b}}^{-1}(0) \cdot \begin{bmatrix} X_{a11} + 1 - E_{0b1} \\ X_{b21} - E_{0b2} \\ X_{b31} - E_{0b3} \end{bmatrix} \end{aligned} \tag{18}$$

where τ_2 is given by using the first rows of two equations in Eq. (18). Finally, we get

$$\mathbf{T}(\mathbf{x_0}) = \mathbf{x_2}. \tag{19}$$

Figure 7(2) shows the Poincaré map obtained by calculating Eqs. (17), (18) and (19). We can observe the bifurcation scenario more clearly.

The Jacobian matrix $\mathbf{DT}$ of the Poincaré map $\mathbf{T}$ can be also derived rigorously from Eqs. (17)–(19). We can calculate the largest Lyapunov exponent by

$$\mu = \lim_{N\to\infty} \frac{1}{N} \sum_{j=1}^{N} \log |\mathbf{DT}_j \cdot e_j| \tag{20}$$

where e_j is a normalized base.

One-parameter bifurcation diagram and the calculated largest Lyapunov exponents are shown in Fig. 9

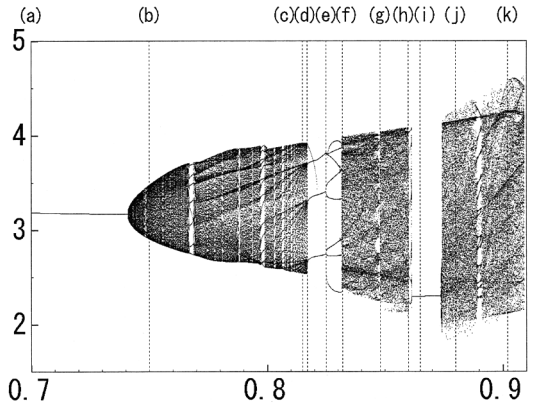

Fig. 9 One-parameter bifurcation diagram. Horizontal: α_b. Vertical: x_{a1}.

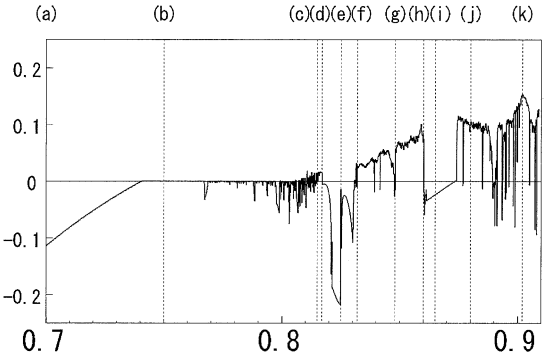

Fig. 10 Largest Lyapunov exponents. Horizontal: α_b. Vertical: μ.

and Fig. 10, respectively. Control parameter is α_b and other parameters are fixed as Fig. 7.

By using these results, we can say the generation of chaos is confirmed numerically and we can describe detailed bifurcation scenario as follows.

One-periodic orbit (a) bifurcates to torus (b) around $\alpha_b = 0.74$. For $0.74 < \alpha_b < 0.805$, we can observe several phase-locked states in torus region. For $0.805 < \alpha_b < 0.817$, the largest Lyapunov exponent becomes positive occasionally though the attractor looks like torus (c), (d). We consider that chaos via folded-torus appears in this interval [12]. For $0.817 < \alpha_b$, chaotic attractors can be observed (f), (h), (j), (k) for almost parameter values except two large periodic windows (e), (i). We can also confirm a lot of small periodic windows are embedded in chaotic region (g).

5. Conclusions

In this paper, we have proposed a chaotic circuit using two RC phase shift oscillators. By using a simpler model of the original circuit, the mechanism of generating chaos has been explained. Further, we have confirmed the generation of chaos by calculating the Lyapunov exponents and have investigated the related bifurcation phenomena.

Our future research is the development of a designing method of chaos-generating circuits based on this study.

References

[1] Special Session on Applications of Chaos in Communications, Proc. ISCAS'97, vol.2, pp.1037–1076, June 1997.
[2] Special Session on Spread Spectrum Communications and Chaos, Proc. ECCTD'97, vol.1, pp.272–341, Aug. 1997.
[3] K. Aihara, T. Takabe, and M. Toyoda, "Chaotic Neural Networks," Physics Lett. A, vol.144, nos.6 and 7, pp.333–340, March 1990.
[4] T. Yamada and K. Aihara, "Chaotic neural network and optimization problems: Complex computational dynamics," Proc. NOLTA'94, pp.157–160, Oct. 1994.
[5] A.L. Zheleznyak and L.O. Chua, "Coexistence of low- and high-dimensional spatiotemporal chaos in a chain of dissipatively coupled Chua's circuits," Int. J. Bifurcation Chaos, vol.4, no.3, pp.639–674, 1994.
[6] Y. Nishio and A. Ushida, "Spatio-temporal chaos in simple coupled chaotic circuits," IEEE Trans. Circuits & Syst. I, vol.42, no.10, pp.678–686, Oct. 1995.
[7] J.M. Cruz and L.O. Chua, "A CMOS IC nonlinear resistor for Chua's circuit," IEEE Trans. Circuits & Syst. I, vol.39, no.12, pp.985–995, Dec. 1992.
[8] M. Delgado-Restituto and A. Rodríguez-Vázquez, "A CMOS Monolithic Chua's Circuit," J. Circuits, Systems, and Computers, vol.3, no.2, pp.259–268, April 1993.
[9] J.M. Cruz and L.O. Chua, "An IC chip of Chua's circuit," IEEE Trans. Circuits & Syst. II, vol.40, no.10, pp.614–625, Oct. 1993.
[10] T. Saito and K. Mitsubori "Chaos due to impulsive switched capacitor," Proc. ECCTD'97, vol.2, pp.1019–1024, 1997.
[11] A. Nedungadi and T.R. Viswanathan, "Design of linear CMOS transconductance elements," IEEE Trans. Circuits & Syst., vol.31, no.10, pp.891–894, Oct. 1984.
[12] N. Inaba and S. Mori, "Folded Torus in the Forced Rayleigh Oscillator with a Diode Pair," IEEE Trans. Circuits & Syst. I, vol.39, no.5, pp.402–411, May 1992.

Yasuteru Hosokawa was born in Hyogo, Japan, on 1974. He received the B.E. and M.E. degrees from Tokushima University, Tokushima, Japan, in 1997, 1999, respectively. He is currently working towards Ph.D. degree at the same university. In 2001, he joined the faculty of Management and Information Science at Shikoku University, Tokushima Japan, where he is currently a research assistant. His research interest is in chaos circuit design. Mr. Hosokawa is a student member of the IEEE.

Yoshifumi Nishio received the B.E., M.E., and Ph.D. degrees in electrical engineering from Keio University, Yokohama Japan, in 1988, 1990, and 1993, respectively. In 1993, he joined the Department of Electrical and Electronic Engineering at Tokushima University, Tokushima Japan, where he is currently an Associate Professor. From May 2000 he is spending a year in the Laboratory of Nonlinear Systems (LANOS) at the Swiss Federal Institute of Technology Lausanne (EPFL) as a visiting professor. His research interests include analysis and application of chaos in electrical circuits, analysis of synchronization in coupled oscillators circuits, development of analyzing methods for nonlinear circuits and theory and application of cellular neural networks. Dr. Nishio is a member of the IEEE.

Akio Ushida received the B.E. and M.E. degrees in electrical engineering from Tokushima University in 1961 and 1966, respectively, and the Ph.D. degree in electrical engineering from University of Osaka Prefecture in 1974. He was an associate professor from 1973 to 1980 at Tokushima University. Since 1980 he has been a Professor in the Department of Electrical Engineering at the university. From 1974 to 1975 he spent one year as a visiting scholar at the Department of Electrical Engineering and Computer Sciences at the University of California, Berkeley. His current research interests include numerical methods and computer-aided analysis of nonlinear systems. Dr. Ushida is a member of IEEE.